Pathways for Extracellular Fenton Chemistry in the Brown Rot Basidiomycete *Gloeophyllum trabeum*

KENNETH A. JENSEN, JR.,[1] CARL J. HOUTMAN,[2] ZACHARY C. RYAN,[1]
AND KENNETH E. HAMMEL[1]*

Institute for Microbial and Biochemical Technology[1] and Fiber Processing and Paper Performance Research Work Unit,[2] U.S. Department of Agriculture Forest Products Laboratory, Madison, Wisconsin 53705

The brown rot fungus *Gloeophyllum trabeum* uses an extracellular hydroquinone-quinone redox cycle to reduce Fe^{3+} and produce H_2O_2. These reactions generate extracellular Fenton reagent, which enables *G. trabeum* to degrade a wide variety of organic compounds. We found that *G. trabeum* secreted two quinones, 2,5-dimethoxy-1,4-benzoquinone (2,5-DMBQ) and 4,5-dimethoxy-1,2-benzoquinone (4,5-DMBQ), that underwent iron-dependent redox cycling. Experiments that monitored the iron- and quinone-dependent cleavage of polyethylene glycol by *G. trabeum* showed that 2,5-DMBQ was more effective than 4,5-DMBQ in supporting extracellular Fenton chemistry. Two factors contributed to this result. First, *G. trabeum* reduced 2,5-DMBQ to 2,5-dimethoxyhydroquinone (2,5-DMHQ) much more rapidly than it reduced 4,5-DMBQ to 4,5-dimethoxycatechol (4,5-DMC). Second, although both hydroquinones reduced ferric oxalate complexes, the predominant form of Fe^{3+} in *G. trabeum* cultures, the 2,5-DMHQ-dependent reaction reduced O_2 more rapidly than the 4,5-DMC-dependent reaction. Nevertheless, both hydroquinones probably contribute to the extracellular Fenton chemistry of *G. trabeum*, because 2,5-DMHQ by itself is an efficient reductant of 4,5-DMBQ.

Basidiomycetes that cause brown rot of wood are the principal recyclers of lignocellulose in coniferous forest ecosystems and also the principal cause of biodegradation of wooden structures. These fungi degrade polysaccharides in wood preferentially but also partially oxidize lignin (6). Because enzymes are too large to penetrate sound wood (1, 9, 32), most researchers believe that brown rotters attack wood polymers by producing small, diffusible, extracellular oxidants that operate at a distance from the hyphae. The oxidative changes that brown rotters cause in cellulose, lignin, and various refractory organic chemicals have led often to the proposal that one of these oxidants is the hydroxyl radical ˙OH (15, 16, 19, 21, 22, 30, 33, 34).

In biological systems, ˙OH is generally produced by the Fenton reaction (Fig. 1, reaction 1). Therefore, to use ˙OH as an oxidant, brown rot fungi need to reduce extracellular Fe^{3+} and produce extracellular H_2O_2. How most of them accomplish this is not well understood, although it has been proposed that cellobiose dehydrogenase (14) or iron-binding catechols (11) could initiate Fenton chemistry by reducing Fe^{3+} outside the fungal mycelium.

We recently identified a quinone redox cycle that the brown rotter *Gloeophyllum trabeum* uses to generate extracellular Fe^{2+} and H_2O_2 (17). *G. trabeum* produces extracellular 2,5-dimethoxyhydroquinone (2,5-DMHQ) (Fig. 2), which reduces Fe^{3+} (Fig. 1, reaction 2). It is implicit that this reaction also yields the 2,5-DMHQ semiquinone radical, which is expected to react reversibly with O_2 to yield 2,5-dimethoxy-1,4-benzoquinone (2,5-DMBQ) and the perhydroxyl radical (˙OOH) (Fig. 1, reaction 3). H_2O_2 is produced when ˙OOH and its

conjugate base, superoxide ($O_2^{˙-}$), dismutate or when either of these oxyradicals is reduced by Fe^{2+} (13). It is also possible, but has not yet been established, that some of the semiquinones reduce Fe^{3+} instead of O_2 (Fig. 1, reaction 4). Finally, the fungal mycelium reduces 2,5-DMBQ to 2,5-DMHQ, thus completing the redox cycle to enable the production of additional Fenton reagent (Fig. 1, reaction 5).

This cycle suffices to generate Fenton reagent in *G. trabeum* cultures (17), but the process in vivo is probably more complex for at least two reasons. First, *G. trabeum* produces not only 2,5-DMHQ but also another hydroquinone, 4,5-dimethoxycatechol (4,5-DMC) (Fig. 2), and is able to reduce a variety of quinones (25). Therefore, it is possible that 4,5-DMC and its oxidized form, 4,5-dimethoxy-1,2-benzoquinone (4,5-DMBQ), undergo an additional redox cycle as described above. Second, *G. trabeum* produces extracellular oxalic acid (7). Oxalate chelates Fe^{3+} strongly (24, 31), and Fe^{3+}-oxalate complexes are relatively poor oxidants whose reactivity with methoxyhydroquinones remains to be determined. To address these questions, we have compared the abilities of the 2,5-DMHQ–2,5-DMBQ and 4,5-DMC–4,5-DMBQ couples to reduce Fe^{3+}-oxalate, to reduce O_2, and to support the generation of extracellular Fenton reagent by *G. trabeum*.

MATERIALS AND METHODS

Reagents. 4,5-DMBQ was prepared by a modified literature method (26). Phenol (1.5 g) and dry powdered copper (100 mg, 150 mesh) were combined with 24 ml of methanol-pyridine (2:1). The mixture was placed in a stoppered flask that was fitted with a balloon. The flask was flushed with O_2, after which it was sealed and the balloon was inflated with about 2.5 liters of O_2. The mixture was stirred at ambient temperature for 3 h and then removed and filtered through a Büchner funnel. The filtrate was concentrated by rotary vacuum evaporation until it was almost dry and then redissolved in methylene chloride-methanol (985:15). It was then applied to a column (57 by 4 cm) of silica gel (SilicAR CC-4 Special; Mallinckrodt), which was developed with the same solvent. Fractions were collected, and those that contained 4,5-DMBQ were identified by compar-

---

* Corresponding author. Mailing address: Institute for Microbial and Biochemical Technology, USDA Forest Products Laboratory, One Gifford Pinchot Dr., Madison, WI 53705. Phone: (608) 231-9528. Fax: (608) 231-9262. E-mail: kehammel@facstaff.wisc.edu.

$$Fe^{2+} + H_2O_2 + H^+ \longrightarrow Fe^{3+} + H_2O + \cdot OH \quad (1)$$

$$H_2Q + Fe^{3+} \rightleftharpoons HQ\cdot + H^+ + Fe^{2+} \quad (2)$$

$$HQ\cdot + O_2 \rightleftharpoons Q + \cdot OOH \quad (3)$$

$$HQ\cdot + Fe^{3+} \rightleftharpoons Q + H^+ + Fe^{2+} \quad (4)$$

$$Q + 2e^- + 2H^+ \longrightarrow H_2Q \quad (5)$$
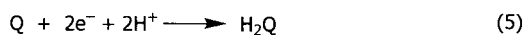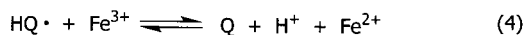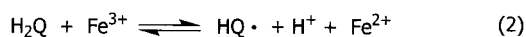
FIG. 1. Reactions of the hydroquinone-driven Fenton system in *G. trabeum*. Q, quinone; H_2Q, hydroquinone; $HQ\cdot$, semiquinone; $\cdot OOH$, perhydroxyl radical.

ing their mobility with that of an authentic 4,5-DMBQ standard, which was kindly donated by P. J. Kersten (USDA Forest Products Laboratory, Madison, Wis.) (18). The crude 4,5-DMBQ thereby obtained was chromatographed again by the same procedure, and the purified compound was recrystallized from methanol to yield 250 to 300 mg of orange needlelike crystals that melted at 228 to 230°C (literature melting point, 226 to 228°C [3]). The mass spectrum, ^1H nuclear magnetic resonance spectrum, and ^{13}C nuclear magnetic resonance spectrum of the product were the same as those reported previously (26).

To prepare 4,5-DMC, 300 mg of 4,5-DMBQ was dissolved in 20 ml of glass-distilled ether and shaken with 20 ml of cold saturated sodium dithionite solution in an acid-washed separatory funnel. The ether phase was kept briefly in an acid-washed beaker under a stream of argon, while the aqueous phase was extracted again with ether. The combined ether phases were then dried over a small column of sodium sulfate and collected in an acid-washed beaker under a stream of argon. The solvent was removed by rotary vacuum evaporation, yielding about 150 mg of yellowish-white crystals that melted at 114 to 115°C (literature melting point, 114°C [3]). The product gave a single peak by gas chromatography. Mass spectrum (m/z): 170 (M^+), 155 ($-CH_3$), 141 ($-HCO$), 127 ($-CH_3$, $-CO$), 109 ($-CH_3$, $-CO$, $-H_2O$). The crystalline 4,5-DMC was stored at -20°C under argon.

Crystalline 2,5-DMBQ was purchased from TCI America. Crystalline 2,5-DMHQ, prepared by reducing 2,5-DMBQ with sodium dithionite as described previously (17), was stored at -20°C under argon. Polyethylene glycol (PEG) labeled with ^{14}C at its terminal hydroxyethyl groups (15.3 mCi g^{-1}, 4,000 molecular weight) was obtained from Amersham. For depolymerization experiments, this [^{14}C]PEG was diluted with unlabeled PEG (4,000 molecular weight) to a specific activity of 0.73 mCi g^{-1}. All other chemicals were commercially available, reagent-grade products.

Organism. For most experiments, *G. trabeum* (ATCC 11539) was grown in stationary 125-ml Erlenmeyer flasks that contained 5 or 6 ml of Kirk's medium with the basal levels of trace elements (20). The carbon source was glucose (55.6 mM), and the nitrogen sources were ammonium nitrate (0.5 mM) and asparagine (0.5 mM). We refer to this medium as medium A. The medium was inoculated with homogenized potato dextrose agar cultures of the fungus (1 g per 100 ml of medium) and incubated at 32°C under air in the dark. The mycelial mats and extracellular medium were used for experiments 7 days after inoculation, at
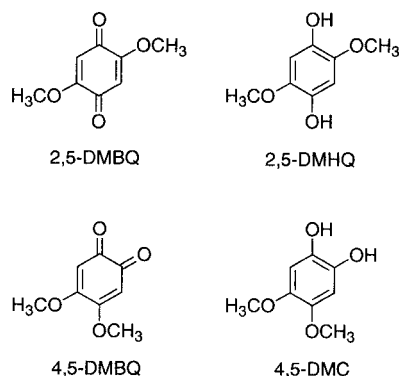
which time the average dry weight of one mat was 10 mg and the average pH of the medium was 4.1. For experiments on PEG cleavage or quinone reduction by *G. trabeum* mycelium, the mats were removed from 50 cultures and shaken gently for 1 h in 1 liter of distilled, deionized water at ambient temperature. The mats were then transferred to fresh water, and the procedure was repeated.

In one experiment to investigate the production of extracellular metabolites, *G. trabeum* was also grown under the conditions described by Paszczynski et al. (25). The cultures were set up in stationary Roux flasks that contained 150 ml of medium A with the following supplements: diammonium tartrate, 1.1 mM; $MnCl_2$, 0.1 mM; and Tween 80, 0.05%. We refer to this medium as medium B. One mycelial mat from a 4-week Roux flask culture was homogenized in 130 ml of sterile water, and this suspension was used to inoculate the cultures (7 ml per 100 ml of medium). The cultures were incubated at 24°C under air in the dark, and the extracellular medium was analyzed 5 weeks after inoculation.

Metabolites in the culture medium. Preliminary experiments showed that the hydroquinones in the extracellular medium of *G. trabeum* cultures were oxidized rapidly if the mycelial mats were disturbed. Therefore, a 250-μl high-performance liquid chromatography (HPLC) syringe was used to obtain samples (200 μl) of medium from the cultures with as little mixing as possible. A 125-μl portion of the sample was purposely oxidized by delivering it into an Eppendorf tube that contained 5 μl of 10 mM $FeCl_3$. Tests with standard solutions of 2,5-DMHQ and 4,5-DMC showed that this procedure converted these substances to their corresponding quinones with >98% yields.

The remaining 75 μl was injected immediately, without filtration, onto a C_{18} reversed-phase HPLC column (Phenomenex Luna; 150 by 4.6 mm, 5-μm particle size). The column was eluted isocratically with water-acetonitrile-formic acid (900:100:1) at 1.5 ml min^{-1} and ambient temperature. The absorbance of the eluate was monitored at 295 nm, a wavelength at which 2,5-DMBQ and 4,5-DMBQ exhibit the same extinction coefficient. The elution times for the metabolites were as follows: 2,5-DMHQ and 4,5-DMC, 6.5 min; 4,5-DMBQ, 7.5 min; and 2,5-DMBQ, 9.5 min.

When the HPLC analysis was completed, 75 μl of the $FeCl_3$-oxidized sample was chromatographed by the same procedure. External standards of 2,5-DMBQ and 4,5-DMBQ were then chromatographed to obtain response factors. The original concentrations of 2,5-DMBQ and 4,5-DMBQ in the medium were calculated from their peak areas in the chromatogram of the untreated sample. The original concentrations of 2,5-DMHQ and 4,5-DMC were then calculated by subtracting these peak areas from the peak areas for 2,5-DMBQ and 4,5-DMBQ in the $FeCl_3$-oxidized sample. This indirect method of determining the hydroquinone concentrations was necessary because we were unable to devise an HPLC protocol that separated 2,5-DMHQ from 4,5-DMC.

Oxalate in the extracellular medium of *G. trabeum* cultures was determined enzymatically with a coupled oxalate oxidase-peroxidase assay according to the manufacturer's instructions (Sigma Chemical Co., St. Louis, Mo.).

Prediction of iron species in solution. Equilibrium constants for the binding of oxalic acid, catechol, and 2,3-dihydroxybenzoic acid to Fe^{3+} were obtained from the National Institute of Standards and Technology database containing critically selected stability constants of metal complexes (31). When several constants for the same equilibrium were shown, the one for the lowest ionic strength was chosen. To model competition between the catecholate species and oxalate for Fe^{3+}, 15 equations, 12 equilibria, and three mass balance equations were solved simultaneously with the SOLVER function of the Microsoft Excel computer program. Since the National Institute of Standards and Technology database contains constants for the association of only a single type of ligand with each cation, the mixed-ligand-species constants were estimated by assuming that, for example, Fe(oxalate)(catechol)$^-$ was formed with a constant whose logarithm is the average of the logarithm of the constant for Fe(catechol)$_2^-$ and the logarithm of the constant for Fe(oxalate)$_2^-$. This is likely to be a poor assumption, but since the mixed species represent a very small fraction of the total chelated species, the resultant error is small.

PEG depolymerization by the mycelium. PEG depolymerization assays were done in 50-ml beakers that each contained 11.0 ml of sodium oxalate buffer (1.0 mM, pH 4.1), two *G. trabeum* mycelial mats, $FeCl_3$ (50 μM), [^{14}C]PEG (330 mg liter^{-1}), and various amounts of quinone. Calculations showed that the oxalate buffer would not scavenge a significant proportion of the $\cdot OH$ produced under these conditions (see data for oxalate and for diethylene glycol at the Notre Dame Radiation Laboratory Radiation Chemistry Data Center [http://allen.rad.nd.edu]). The reaction mixtures were rotary shaken at 200 rpm and ambient temperature for 2 h in the dark. The extracellular pH increased an average of 0.2 units during this time. Samples (200 μl) were taken from triplicate reaction mixtures at 1 and 2 h, and each was filtered through a 0.45-μm-pore-size membrane. More than 99% of the ^{14}C in the sample was recovered by this procedure. A portion (150 μl) of each filtrate was analyzed by gel permeation chromatog-

FIG. 2. Structures of the hydroquinones and quinones investigated.

raphy (GPC) and scintillation counting of the collected fractions as described previously (17). The column was calibrated beforehand with PEG standards of known molecular weight, also as previously described (17).

Calculation of the number of chain scissions in PEG. Because commercially available [14C]PEG is labeled only on the ends of the polymer, its scission yields significant quantities of unlabeled polymer that are silent when analyzed by our GPC procedure. As the reaction progresses, the difference between the molecular weight distributions of the labeled and unlabeled material first increases and then decreases. To address this problem, we obtained the relationship between the true molecular weight and the molecular weight of the labeled material by computer simulation. The program was written in Visual Basic for Microsoft Excel and is available from the authors upon request.

From the specific activity and molecular weight of the PEG, we determined that it had, on average, one 14C-labeled end group per polymer molecule. We assumed that these end groups were distributed with relative frequencies of 1:2:1 among molecules with zero, one, or two labeled end groups, respectively. In the simulation, 10^5 linear molecules were defined with the same molecular weight distribution as the undegraded PEG, and then changes in the molecular weight distributions of the labeled and unlabeled materials were monitored during 6×10^5 random scission events. From this simulation, we developed an empirical model to determine the true molecular weight from the GPC data. Comparisons of the simulated GPC data with the experimental data showed that they corresponded closely, so our assumption of random chain scission in experimental samples appears to be correct. The average number of scissions (n) per polymer was calculated from the equation $n = (M_n^0/M_n^t) - 1$, where M_n^0 is the true number average molecular weight at time zero and M_n^t is the true number average molecular weight at time t.

Fe^{3+} reduction by the hydroquinones. Acid-washed glassware and Milli-Q water were used to prepare all solutions, and all operations were conducted in dim light. Stock solutions of 2,5-DMHQ and 4,5-DMC (2.0 mM) were prepared in 1.0 mM sodium oxalate (final pH, 4.1) under argon. A stock solution of FeCl$_3$ (1.0 mM) was prepared in 2.0 mM sodium oxalate (final pH, 4.1), also under argon. For anoxic reactions, 65.0 ml of argon-saturated sodium oxalate buffer (1.0 mM, pH 4.1) and 30.0 ml of argon-saturated FeCl$_3$ stock solution were added at 25°C to a stirred, water-jacketed beaker, which was kept under a stream of argon. The reaction was initiated by adding one of the anoxic hydroquinone stock solutions (5.0 ml) to give initial concentrations of 300 μM Fe^{3+} and 100 μM hydroquinone in 1.3 mM sodium oxalate buffer. Samples (1.5 ml) were removed at various time and were mixed rapidly with an equal volume of 4.0 mM bathophenanthroline disulfonic acid (BPS) in 200 mM sodium oxalate (pH 4.1). The absorbance at 535 nm was read immediately, and an extinction coefficient of 22.1 mM^{-1} cm^{-1} was used to calculate the amount of Fe^{2+} formed (2). Oxic reactions were performed in the same way, except that the hydroquinone stock solutions were the only ones kept under argon.

Additional reactions were run in the presence of BPS under anoxic conditions to determine the stoichiometry of Fe^{3+} reduction by the hydroquinones under irreversible conditions. The reaction mixtures contained FeCl$_3$ (100 μM), 2,5-DMHQ or 4,5 DMC (26 μM), and BPS (2.0 mM) in 3.0 ml of sodium oxalate buffer (1.1 mM; final pH, 4.1) and were constantly stirred. The hydroquinones were used to start the reactions, which were monitored at 535 nm in a Hitachi U-3010 double-beam, monochromator-equipped UV/visible spectrum spectrophotometer. We observed that if the reactions were done instead in a diode-array-equipped spectrophotometer, the greater intensity of incident light resulted in a slow but detectable photoreduction of the Fe^{3+}-oxalate.

Iron-dependent O$_2$ reduction by the hydroquinones and quinones. O$_2$ uptake was determined with a Yellow Springs Instruments model 5300 oxygen electrode. Solutions were prepared as described for the oxic Fe^{3+} reduction experiments and were equilibrated to 25°C before use. The reactions (1.8-ml reaction volumes) were conducted in dim light at 25°C in a stirred, water-jacketed glass chamber that had been washed with acid beforehand. Control reactions without iron were always performed before iron-containing reactions. For complete hydroquinone-dependent reactions, 1,170 μl of air-saturated sodium oxalate buffer (1.0 mM, pH 4.1) and 540 μl of air-saturated FeCl$_3$ solution were added to the cell. A portion of the anoxic hydroquinone stock solution was then vortexed briefly in an acid-washed Eppendorf tube to oxygenate it, and 90 μl was injected into the cell to start the reaction. This procedure gave initial concentrations of 300 μM Fe^{3+} and 100 μM hydroquinone in 1.3 mM sodium oxalate buffer (final pH, 4.1). Reverse reactions were conducted similarly, with 100 μM quinone instead of 100 μM hydroquinone and with 200 μM FeCl$_2$ in place of 300 μM FeCl$_3$. Control reactions contained oxalate buffer of the appropriate concentration in place of the hydroquinone, quinone, or iron solution.

Reduction of 2,5-DMBQ and 4,5-DMBQ by *G. trabeum*. Each assay mixture used for determination of 2,5-DMBQ or 4,5-DMBQ reduction contained three
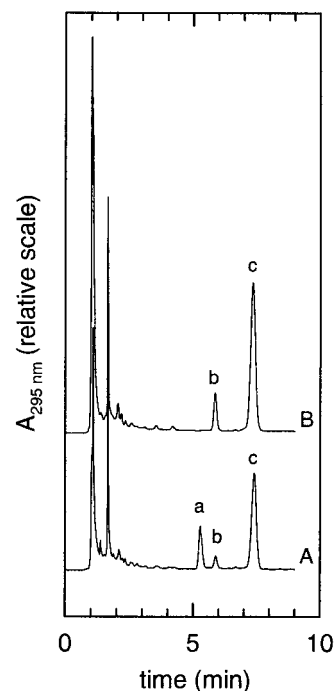
FIG. 3. HPLC analysis of extracellular metabolites from *G. trabeum* cultures. (A) Untreated sample; (B) sample oxidized with FeCl$_3$. The labeled peaks consisted of 2,5-DMHQ plus 4,5-DMC (a), 4,5-DMBQ (b), and 2,5-DMBQ (c).

G. trabeum mycelial mats and 50 μM quinone in 18.0 ml of sodium oxalate buffer (1.0 mM, pH 4.1). Preliminary experiments showed that this buffer sufficed to maintain the pH at 4.1 ± 0.1 for more than 1 h. In some assays, 1 mM desferrioxamine was also added to minimize iron-catalyzed cycling of the hydroquinone-quinone couples. The reductions were done in acid-washed 50-ml beakers, which were rotary shaken at 200 rpm and ambient temperature in the dark. Samples (100 μl) were withdrawn with an HPLC syringe at time zero and every 7 min thereafter. They were injected immediately, without filtration, onto the Phenomenex Luna HPLC column described above. The column was eluted with water-acetonitrile-formic acid (850:150:1) at 1.5 ml min^{-1} and ambient temperature. Each hydroquinone-quinone pair was separated with baseline resolution. Their retention times were as follows: 2,5-DMHQ, 3.2 min; 2,5-DMBQ, 4.1 min; 4,5-DMC, 3.2 min; and 4,5-DMBQ, 3.4 min. External standards of the four metabolites were used to obtain response factors for quantitation.

Reduction of 4,5-DMBQ by 2,5-DMHQ. Solutions used to measure the reduction of 4,5-DMBQ by 2,5-DMHQ were prepared as described above for the Fe^{3+} reduction experiments. The reaction was monitored in a Shimadzu 1501 diode-array UV/visible spectrophotometer. The reaction mixture contained 2,5-DMHQ (150 μM), 4,5-DMBQ (150 μM), and sodium oxalate buffer (1.0 mM, pH 4.1) in a final volume of 3.0 ml. The reaction mixture was stirred at 25°C in an acid-washed, 1-cm-path-length quartz cell, and spectra were recorded for 1.5 min at 10-s intervals. The spectrum at zero time was reconstructed from pure component spectra of 2,5-DMHQ and 4,5-DMBQ.

RESULTS AND DISCUSSION

Extracellular quinonoid metabolites of *G. trabeum*. We confirmed the observation of Paszczynski et al. that *G. trabeum* produces not only an extracellular *p*-hydroquinone, 2,5-DMHQ, but also an extracellular catechol, 4,5-DMC (25). In addition, we observed the corresponding quinones, 2,5-DMBQ and 4,5-DMBQ (Fig. 3; Table 1). In 7-day cultures grown in medium A under previously described conditions (17), and also in 5-week cultures grown in medium B under the conditions described by Paszczynski et al. (25), the ratio of 2,5-

TABLE 1. Oxidized and reduced forms of quinones in
G. trabeum cultures

Metabolites present	Concn $(\mu M)^a$	Mean % in reduced form
In medium A		
2,5-DMBQ + 2,5-DMHQ	27.6 ± 3.9	44^b
4,5-DMBQ + 4,5-DMC	4.1 ± 0.6	73^b
In medium B		
2,5-DMBQ + 2,5-DMHQ	39.4 ± 4.1	65^c
4,5-DMBQ + 4,5-DMC	7.6 ± 0.8	92^c

^{a} Means $\pm$ SDs for four replicates (medium A) or duplicates (medium B).
^{b} Different by t test with $P = 0.013$.
^{c} Different by t test with $P = 0.004$.

DMBQ plus 2,5-DMHQ to 4,5-DMBQ plus 4,5-DMC was greater than 5:1. However, the 4,5-dimethoxy metabolite was significantly more reduced than the 2,5-dimethoxy metabolite (Table 1).

Extracellular Fe^{3+} chelators of *G. trabeum*. The extracellular concentration of oxalate (mean $\pm$ the standard deviation) in our 7-day cultures was 500 ± 150 μM ($n = 4$). In addition, the cultures produced some unidentified, polar, UV-absorbing metabolites (Fig. 3), some of which might be Fe^{3+}-binding catechols of the type reported earlier by Goodell et al. (11). With the exception of 4,5-DMC, these catechols have not been described in detail, but they are thought to bind Fe^{3+} through two vicinal phenolate groups (as in catechol) or through vicinal phenolate and benzoate groups (as in 2,3-dihydroxybenzoic acid).

To compare how oxalate and catechols might contribute to Fe^{3+} chelation in *G. trabeum* cultures, we assumed that all of the unidentified UV-absorbing material in the chromatogram of Fig. 3A (including the void-volume peak) consisted of compounds with properties similar to those of catechol or 2,3-dihydroxybenzoic acid. It was then possible to calculate that the *G. trabeum* cultures we used contained no more than a 500 μM concentration of unidentified catecholic compounds.

We used published binding constants (31) to estimate the concentrations of Fe^{3+} chelates that would be present if 20 μM Fe^{3+}, 500 μM oxalate, and 500 μM 2,3-dihydroxybenzoate or catechol were present simultaneously. The results show that although both catechols compete effectively with oxalate as Fe^{3+} chelators at neutral pH, neither of them does at pH 4.1, the pH value found in *G. trabeum* cultures (Table 2). Therefore, we concluded that oxalate, rather than a catechol, was the dominant chelator of Fe^{3+} under our culture conditions.

Efficacy of the quinones in the extracellular Fenton system. To compare $\cdot OH$ generation by the 2,5-DMHQ–2,5-DMBQ and 4,5-DMC–4,5-DMBQ couples, we measured the rate of PEG depolymerization by *G. trabeum* mycelium in the presence of Fe^{3+}, dilute oxalate, and each of the quinones. PEG is a useful target molecule for assays of extracellular Fenton reagent because it does not penetrate cell membranes (23, 28, 29) and because it is cleaved by strongly oxidizing radicals that abstract aliphatic hydrogens (5, 10, 12, 16).

The data showed that both quinones supported PEG cleavage, but the reaction with 4,5-DMBQ was significantly slower than the reaction with 2,5-DMBQ, even when 4,5-DMBQ was supplied at concentrations higher than those found in *G. tra-*

TABLE 2. Predicted chelates of Fe^{3+} (20 μM) in the presence of
500 μM oxalate and a 500 μM concentration of the
indicated catechol

Chelate^a	Concn (μM)			
	1,2-Dihydroxybenzene dianion		2,3-Dihydroxybenzoic acid dianion	
	pH 7.0	pH 4.1	pH 7.0	pH 4.1
$Fe(ox)^+$	0.00	0.00	0.00	0.00
$Fe(ox)_2^-$	0.00	1.09	0.24	1.09
$Fe(ox)_3^{3-}$	0.03	18.91	7.11	18.91
$Fe(cat)^+$	0.01	0.00	12.65	0.00
$Fe(cat)_2^-$	19.89	0.00	0.00	0.00
$Fe(cat)_3^{3-}$	0.06	0.00	0.00	0.00
$Fe(ox)(cat)^-$	0.00	0.00	0.00	0.00
$Fe(ox)_2(cat)^{3-}$	0.00	0.00	0.00	0.00
$Fe(ox)(cat)_2^{3-}$	0.00	0.00	0.00	0.00

^{a} Abbreviations: ox, oxalate; cat, catechol.

beum cultures (Table 3). We also examined PEG cleavage with both quinones present simultaneously at physiological concentrations, but we found no evidence that they acted synergistically. No PEG cleavage occurred when the quinones were omitted. We did not perform controls without Fe^{3+} because our previous data already showed that it is essential for the reaction to proceed (17).

When reactions 2 through 5 (Fig. 1) are considered, it is evident that there are three possible explanations for these results. First, 4,5-DMC might reduce Fe^{3+} more slowly than 2,5-DMHQ does (reaction 2 and possibly reaction 4). Second, the 4,5-DMC semiquinone might reduce O_2, and thus produce H_2O_2, more slowly than the 2,5-DMHQ semiquinone does (reaction 3). Finally, the fungal mycelium might reduce 4,5-DMBQ more slowly than it reduces 2,5-DMBQ (reaction 5). The experiments described below were designed to assess each of these possibilities.

Reduction of Fe^{3+} by 2,5-DMHQ and 4,5-DMC. First, we determined the stoichiometries of Fe^{3+} reduction by 2,5-DMHQ and 4,5-DMC in 1.1 mM oxalate buffer, with the reactions being conducted under argon in the presence of the colorimetric Fe^{2+} chelator BPS. Under these conditions, Fe^{3+} reduction by the hydroquinones is expected to be irreversible and O_2 is unavailable to react with the resulting semiquinones. Each hydroquinone reduced 1.96 to 1.98 equivalents of Fe^{3+} within 1 min in this experiment (data not shown). Therefore,

TABLE 3. Cleavage of [^{14}C]PEG by *G. trabeum* mycelial mats

Quinone(s) added (concn)	Scissions/polymer^a at:	
	1 h	2 h
None	-0.013 ± 0.007	-0.029 ± 0.007
2,5-DMBQ (28 μM)	0.309 ± 0.021	0.771 ± 0.013
4,5-DMBQ (4 μM)	0.087 ± 0.020	0.215 ± 0.034
2,5-DMBQ (28 μM) + 4,5-DMBQ (4 μM)	0.397 ± 0.024	0.831 ± 0.079
2,5-DMBQ (32 μM)	$0.377^b \pm 0.054$	$0.745^c \pm 0.055$
4,5-DMBQ (32 μM)	$0.110^b \pm 0.015$	$0.221^c \pm 0.043$

^{a} Means $\pm$ SDs for three replicates.
^{b} Different by t test with $P = 0.0012$.
^{c} Different by t test with $P = 0.0002$.
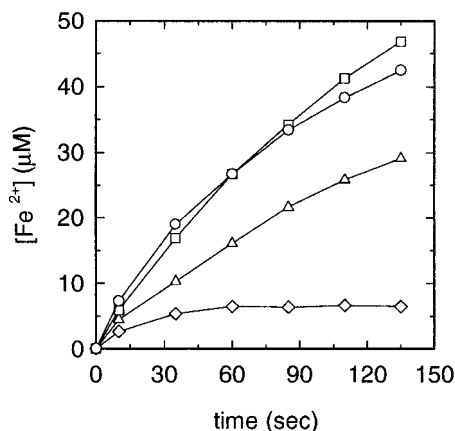
FIG. 4. Fe^{3+} reduction by 2,5-DMHQ under argon ($\triangle$), by 2,5-DMHQ under air ($\diamond$), by 4,5-DMC under argon ($\square$), and by 4,5-DMC under air ($\bigcirc$). In the oxic reactions, the levels of Fe^{2+} declined with time (not shown). In the anoxic reactions, the Fe^{2+} stabilized at a concentration of 120 μM when 2,5-DMHQ was the reductant and at 70 μM when 4,5-DMC was the reductant. The difference between these final hydroquinone concentrations indicates that the standard $2e^-$ reduction potential of the 2,5-DMHQ–2,5-DMBQ couple is 32 mV more negative than that of the 4,5-DMC–4,5-DMBQ couple, in good agreement with the published difference of 37 mV (4, 8).

the potential reductants of Fe^{3+} in the *G. trabeum* system include not only 2,5-DMHQ and 4,5-DMC (reaction 2) but also their corresponding semiquinones (reaction 4).

Next, we compared the rates at which 2,5-DMHQ and 4,5-DMC reduced Fe^{3+} in 1.3 mM oxalate under anoxic conditions. We omitted BPS from the reaction mixtures because colorimetric Fe^{2+} chelators affect the reaction rates when they are present during Fe^{3+} reductions (2). Instead, we obtained samples at intervals during the reaction and mixed them rapidly with concentrated oxalate buffer and BPS, after which the absorbances were read immediately. This approach was based on our prior observation that the rate of Fe^{3+} reduction by the hydroquinones was inhibited more than 95% by 100 mM oxalate (data not shown). Although we were unable to take measurements rapidly enough to obtain linear initial rates, it is evident from the results (Fig. 4) that 4,5-DMC reduces Fe^{3+} in anoxic, dilute oxalate at pH 4.1 somewhat more rapidly than 2,5-DMHQ does. Therefore, the relatively low efficiency of the 4,5-DMC-driven Fenton system (Table 3) cannot be attributed to a lower rate of reaction between 4,5-DMC and Fe^{3+} (reactions 2 and 4).

Finally, we measured the rates at which 2,5-DMHQ and 4,5-DMC reduced Fe^{3+} in the same buffer under air. Under these conditions, Fe^{3+} is expected to be the only efficient oxidant of the initial hydroquinones (reaction 2) (27), but O_2 (reaction 3) can compete with Fe^{3+} (reaction 4) as an oxidant of the semiquinones (13). As a result, the oxic reaction will generate some $\cdot OOH$ in place of Fe^{2+}, and some of this $\cdot OOH$ will oxidize additional Fe^{2+} rapidly, thereby generating H_2O_2 (13). This H_2O_2 will consume yet more Fe^{2+} in the Fenton reaction (reaction 1), which is rapid when oxalate is the ligand of Fe^{2+} (24). Therefore, if O_2 oxidizes the semiquinones efficiently, one would expect a lower rate of Fe^{2+} accumulation under air than under argon. The data (Fig. 4) showed that O_2
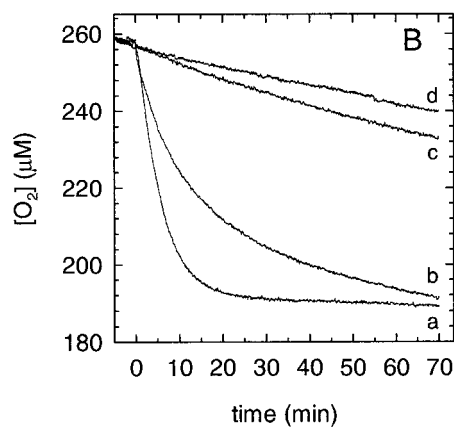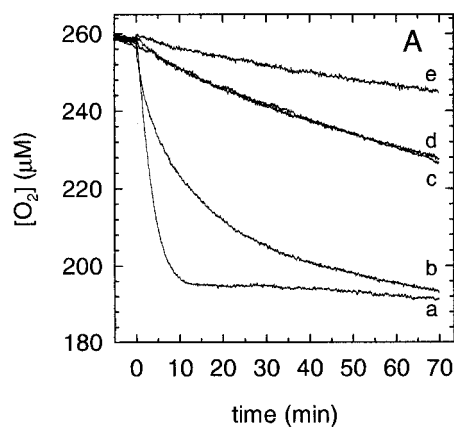
FIG. 5. O_2 reduction by the hydroquinone-quinone couples in the presence of iron. (A) With hydroquinone and Fe^{3+}. The curves show O_2 uptake with 2,5-DMHQ plus Fe^{3+} (a), with 4,5-DMC plus Fe^{3+} (b), with 2,5-DMHQ minus Fe^{3+} (c), with 4,5-DMC minus Fe^{3+} (d), and with Fe^{3+} minus hydroquinone (e). (B) With quinone and Fe^{2+}. The curves show O_2 uptake with 2,5-DMBQ plus Fe^{2+} (a), with 4,5-DMBQ plus Fe^{2+} (b), with Fe^{2+} minus quinone (c), and with oxalate buffer alone (d).

markedly inhibited the initial rate of Fe^{3+} reduction by 2,5-DMHQ but had little effect on the initial rate of Fe^{3+} reduction by 4,5-DMC. This result suggested that the 2,5-DMHQ semiquinone reacts with O_2 (reaction 3) more rapidly than the 4,5-DMC semiquinone does.

Reduction of O_2 by 2,5-DMHQ and 4,5-DMC. The results of O_2 electrode experiments were consistent with the above-stated hypothesis. In 1.3 mM oxalate buffer at pH 4.1, the reaction of 2,5-DMHQ with Fe^{3+} consumed O_2 more rapidly than the reaction of 4,5-DMC with Fe^{3+} (Fig. 5A, curves a and b). Neither hydroquinone reacted rapidly with O_2 in the absence of added Fe^{3+} (curves c and d), and the uptake that did occur was probably attributable to contamination of the reagents with Fe^{3+}. This result agrees with the general rule that nonradical species react very slowly with diradical O_2 (27). The low rate of O_2 uptake that we observed in the absence of hydroquinone (curve e) probably resulted from a photoreaction between oxalate and Fe^{3+} (14).

Further experiments showed that these reactions were reversible; i.e., the quinones could be used to oxidize Fe^{2+} with concomitant O_2 consumption. O_2 uptake was considerably
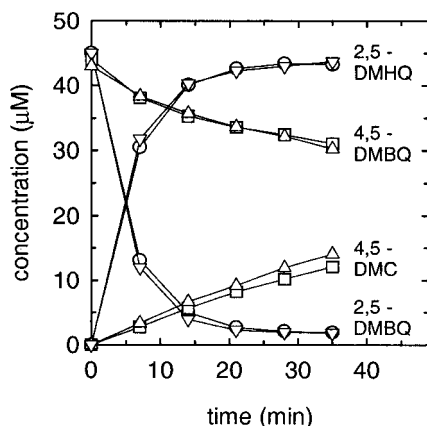
FIG. 6. Reduction of 2,5-DMBQ and 4,5-DMBQ by *G. trabeum*. The curves show results obtained in four separate incubations: increase in 2,5-DMHQ and decrease in 2,5-DMBQ in the presence of desferrioxamine (○), increase in 2,5-DMHQ and decrease in 2,5-DMBQ in the absence of desferrioxamine (▽), increase in 4,5-DMC and decrease in 4,5-DMBQ in the presence of desferrioxamine (□), and increase in 4,5-DMC and decrease in 4,5-DMBQ in the absence of desferrioxamine (△). This experiment was repeated with different mycelial mats and gave essentially the same results (data not shown).

FIG. 7. Spectrophotometric observation of 4,5-DMBQ reduction by 2,5-DMHQ. The arrows indicate the directions of change in absorbance. The final spectrum was the same as that exhibited by 150 μM 2,5-DMBQ plus 150 μM 4,5-DMC.

faster with 2,5-DMBQ than it was with 4,5-DMBQ (Fig. 5B, curves a and b), which again suggests that the 2,5-DMHQ semiquinone reacts with O_2 more rapidly than the 4,5-DMC semiquinone does. The autoxidation of Fe^{2+}-oxalate (curve c) and the photoreaction of oxalate with contaminating Fe^{3+} (curve d) made relatively small contributions to these O_2 uptake rates.

In sum, these results indicate that the extracellular hydroquinones of *G. trabeum* generate Fenton reagent by the iron-dependent pathways of reactions 2 to 4 (Fig. 1). Although 4,5-DMC reduces Fe^{3+} more rapidly than 2,5-DMHQ does via reaction 2, it reduces O_2 more slowly via reaction 3, and consequently there is insufficient H_2O_2 to react with the Fe^{2+} that accumulates in place of ·OOH via reaction 4. These results explain, in part, why 2,5-DMBQ supports more rapid PEG cleavage than 4,5-DMBQ does.

Reduction of 2,5-DMBQ and 4,5-DMBQ by *G. trabeum*. Reduction of the quinones (Fig. 1, reaction 5) is the step that drives *G. trabeum* extracellular Fenton chemistry. We had already observed that the fungal mycelium reduces 2,5-DMBQ rapidly (17), and it seemed reasonable that 4,5-DMBQ might be reduced likewise. However, we found that the rate of 4,5-DMBQ reduction by fungal mycelium (in 1.0 mM oxalate, pH 4.1) was much lower than the rate of 2,5-DMBQ reduction (Fig. 6). This result cannot be attributed to a rapid reoxidation of 4,5-DMC by contaminating Fe^{3+}, because the rate of reduction was unaffected by desferrioxamine (1 mM), which forms with Fe^{3+} a tight complex that is inert to most reductants (13). These data provide an additional explanation for the low rate of 4,5-DMBQ-supported PEG cleavage that we observed in the experiment described in Table 3.

Reduction of 4,5-DMBQ by 2,5-DMHQ. Even though the *G. trabeum* mycelium reduced 4,5-DMBQ more slowly than it reduced 2,5-DMBQ, it was evident that the fungus was able to maintain the 4,5-DMC–4,5-DMBQ couple in a more reduced
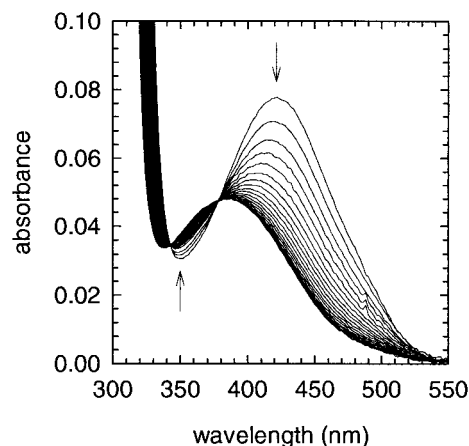
state than it maintained the 2,5-DMHQ–2,5-DMBQ couple (Table 1). The only likely explanation appeared to be that 2,5-DMHQ, rather than the mycelium, was reducing 4,5-DMBQ in fungal cultures. Spectrophotometric experiments confirmed that 2,5-DMHQ reduced 4,5-DMBQ rapidly and quantitatively in 1.0 mM oxalate buffer without any requirement for mycelium or exogenous Fe^{3+} (Fig. 7).

The most obvious route for this oxidoreduction is one that is catalyzed by contaminating Fe^{3+} in the reagents; i.e., 2,5-DMHQ reduces Fe^{3+}, and the resulting Fe^{2+} then reduces 4,5-DMBQ. However, we found that the reaction between 2,5-DMHQ and 4,5-DMBQ was not stimulated by 50 μM Fe^{3+} and was inhibited only slightly by 1 mM desferrioxamine (data not shown). Therefore, we suspect that the redox reaction between 2,5-DMHQ and 4,5-DMBQ is chiefly iron independent. One possibility is that it proceeds via hydride transfer within mixed quinhydrone complexes between 2,5-DMHQ and 4,5-DMBQ (35).

Summary of the pathways for quinone reduction. Even though 4,5-DMBQ is a poor substrate for the mycelial quinone-reducing system of *G. trabeum*, the rapid reduction of this quinone by 2,5-DMHQ provides a route for the formation of 4,5-DMC. The fungus evidently can reduce 4,5-DMBQ directly (Fig. 6), but we cannot rule out the possibility that our washed mycelium contained some bound 2,5-DMBQ. Therefore, we suspect that 4,5-DMBQ is primarily reduced outside the mycelium through a 2,5-DMHQ–2,5-DMBQ redox shuttle. 2,5-DMBQ is presumably reduced to 2,5-DMHQ by a mycelial quinone reductase, which we are presently attempting to identify.

Implications for wood decay. It remains unclear whether there is a mechanistic reason for the production of two extracellular hydroquinone-quinone couples by *G. trabeum*, but it is possible that the fungus uses them to modulate the reactivity of its Fenton system. When the 2,5-DMHQ-driven reaction operates alone in air, it generates enough ·OOH and H_2O_2 to oxidize all of the Fe^{2+}-oxalate that it produces (Fig. 4), and these oxidations occur rapidly, with rate constants of $10^4 \ M^{-1}$

s^{-1} or higher (13, 24). Under these conditions, the Fenton reaction probably occurs near the site where 2,5-DMHQ first reduces Fe^{3+}-oxalate. By contrast, excess Fe^{2+}-oxalate is produced if the 4,5-DMC-driven reaction operates (Fig. 4). Because it autooxidizes with a rate constant of less than $10\ M^{-1}$ s^{-1} at pH 4 (24), Fe^{2+}-oxalate may diffuse to more remote locations, where it could initiate Fenton chemistry by reducing 2,5-DMBQ or 4,5-DMBQ. Even if the quinones are unavailable, Fe^{2+}-oxalate autooxidation will lead to slow ·OH production, as proposed by Hyde and Wood (14).

Wood's group has already pointed out that secreted oxalic acid tends to protect the hyphae of brown rot fungi from oxidative damage because Fe^{2+}-oxalate autooxidation is slow at low pH (14, 24). Our results suggest that two additional protective mechanisms probably operate in the *G. trabeum* system. First, a low pH in the hyphal vicinity will inhibit the reduction of Fe^{3+} by 2,5-DMHQ and 4,5-DMC because protons are products of these reactions (Fig. 1, reactions 2 and 4). Second, a high oxalate concentration near the hyphae will inhibit Fe^{3+} reduction by the hydroquinones, because when oxalate is present in excess at pH 4, almost all of the Fe^{3+} is present as $Fe(oxalate)_3^{3-}$, which has a standard $1e^-$ reduction potential (E^0) of -121 mV (24). This value is considerably more negative than those expected for typical methoxyhydroquinones and methoxysemiquinones (13). By contrast, methoxyhydroquinones and methoxysemiquinones are expected to be better reductants of $Fe(oxalate)_2^-$ ($E^0 = +181$ mV) and $Fe(oxalate)^+$ ($E^0 = +430$ mV), which will be more abundant in dilute oxalate at a distance from the hyphae (24).

ACKNOWLEDGMENTS

REFERENCES

1. **Blanchette, R. A., E. W. Krueger, J. E. Haight, M. Akhtar, and D. E. Akin.** 1996. Cell wall alterations in loblolly pine wood decayed by the white-rot fungus *Ceriporiopsis subvermispora*. J. Biotechnol. **53:**203–213.
2. **Cowart, R. E., F. L. Singleton, and J. S. Hind.** 1993. A comparison of bathophenanthrolinedisulfonic acid and ferrozine as chelators of iron(II) in reduction reactions. Anal. Biochem. **211:**151–155.
3. **Dallacker, F., and G. Löhnert.** 1972. Synthesen substituierter 4,5-Methylendioxy-benzochinone-(1,2). Chem. Ber. **105:**1586–1594.
4. **Dallacker, F., G. Löhnert, and I. Kim.** 1974. Notiz über Redoxpotentiale substituierter 4,5-Methylendioxy-1,2-benzochinone. Chem. Ber. **107:**2415–2417.
5. **Decker, C., and J. Marchal.** 1969. Importance des réactions intramoléculaires au cours de l'autoxydégradation du polyoxyéthylène à 25°C. Etude par amorçage radiochimique indirect en solution aqueuse diluée, p. 231–237. *In* Kinetics and mechanism of polyreactions, vol. 5. Akadémiai Kiadó, Budapest, Hungary.
6. **Eriksson, K.-E. L., R. A. Blanchette, and P. Ander.** 1990. Microbial and enzymatic degradation of wood and wood components. Springer-Verlag, Berlin, Germany.
7. **Espejo, E., and E. Agosin.** 1991. Production and degradation of oxalic acid by brown rot fungi. Appl. Environ. Microbiol. **57:**1980–1986.
8. **Flaig, W., H. Beutelspacher, H. Riemer, and E. Kälke.** 1968. Einfluß von Substituenten auf das Redoxpotential substituierter Benzochinone-(1,4). Liebigs Ann. Chem. **719:**96–111.
9. **Fluornoy, D. S., T. K. Kirk, and T. L. Highley.** 1991. Wood decay by brown-rot fungi: changes in pore structure and cell wall volume. Holzforschung **45:**383–388.
10. **Gondet, J. C., C. Crouzet, and J. Marchal.** 1969. Etude du mécanisme de la décomposition monomoléculaire des radicaux péroxyles formés sur le polyoxyéthylène au cours de l'autoxydation amorcée en solution chloroformique ou aqueuse diluée par irradiation γ à 25°C, p. 249–254. *In* Kinetics and mechanism of polyreactions, vol. 5. Akadémiai Kiadó, Budapest, Hungary.
11. **Goodell, B., J. Jellison, J. Liu, G. Daniel, A. Paszczynski, F. Fekete, S. Krishnamurthy, L. Jun, and G. Xu.** 1997. Low molecular weight chelators and phenolic compounds isolated from wood decay fungi and their role in the fungal biodegradation of wood. J. Biotechnol. **53:**133–162.
12. **Gugumus, G., and J. Marchal.** 1968. Radiolyse oxydante du polyoxyéthylèneglycol en solution chloroformique diluée. J. Polym. Sci. C 3963–3972.
13. **Halliwell, B., and J. M. C. Gutteridge.** 1999. Free radicals in biology and medicine, 3rd ed. Oxford University Press, Oxford, United Kingdom.
14. **Hyde, S. M., and P. Wood.** 1997. A mechanism for production of hydroxyl radicals by the brown-rot fungus *Coniophora putanea*: Fe(III) reduction by cellobiose dehydrogenase and Fe(II) oxidation at a distance from the hyphae. Microbiology **143:**259–266.
15. **Jin, L., T. P. Schultz, and D. D. Nicholas.** 1990. Structural characterization of brown-rotted lignin. Holzforschung **44:**133–138.
16. **Kerem, Z., W. Bao, and K. E. Hammel.** 1998. Rapid polyether cleavage via extracellular one-electron oxidation by a brown-rot basidiomycete. Proc. Natl. Acad. Sci. USA **95:**10373–10377.
17. **Kerem, Z., K. A. Jensen, and K. E. Hammel.** 1999. Biodegradative mechanism of the brown rot basidiomycete *Gloeophyllum trabeum*: evidence for an extracellular hydroquinone-driven Fenton reaction. FEBS Lett. **446:**49–54.
18. **Kersten, P. J., B. Kalyanaraman, K. E. Hammel, B. Reinhammar, and T. K. Kirk.** 1990. Comparison of lignin peroxidase, horseradish peroxidase and laccase in the oxidation of methoxybenzenes. Biochem. J. **268:**475–480.
19. **Kirk, T. K.** 1975. Effects of a brown-rot fungus, *Lenzites trabea*, on lignin in spruce wood. Holzforschung **29:**99–107.
20. **Kirk, T. K., S. Croan, M. Tien, K. E. Murtagh, and R. L. Farrell.** 1986. Production of multiple ligninases by *Phanerochaete chrysosporium*: effect of selected growth conditions and use of a mutant strain. Enzyme Microb. Technol. **8:**27–32.
21. **Kirk, T. K., R. Ibach, M. D. Mozuch, A. H. Conner, and T. L. Highley.** 1991. Characteristics of cotton cellulose depolymerized by a brown-rot fungus, by acid, or by chemical oxidants. Holzforschung **45:**239–244.
22. **Koenigs, J. W.** 1974. Hydrogen peroxide and iron: a proposed system for decomposition of wood by brown-rot basidiomycetes. Wood Fiber **6:**66–79.
23. **Money, N. P.** 1990. Measurement of pore size in the hyphal cell wall of *Achlya bisexualis*. Exp. Mycol. **14:**234–242.
24. **Park, J. S. B., P. M. Wood, M. J. Davies, B. C. Gilbert, and A. C. Whitwood.** 1997. A kinetic and ESR investigation of iron(II) oxalate oxidation by hydrogen peroxide and dioxygen as a source of hydroxyl radicals. Free Radic. Res. **27:**447–458.
25. **Paszczynski, A., R. Crawford, D. Funk, and B. Goodell.** 1999. De novo synthesis of 4,5-dimethoxycatechol and 2,5-dimethoxyhydroquinone by the brown rot fungus *Gloeophyllum trabeum*. Appl. Environ. Microbiol. **65:**674–679.
26. **Prati, L., and M. Rossi.** 1995. A simple route to 4,5-dialkoxy-*o*-quinones by catalytic oxidation of phenol. Gazz. Chim. Ital. **125:**83–86.
27. **Roginsky, V. A., L. M. Pisarenko, W. Bors, and C. Michel.** 1999. The kinetics and thermodynamics of quinone-semiquinone-hydroquinone systems under physiological conditions. J. Chem. Soc. Perkin Trans. **2:**871–876.
28. **Scherrer, R., and P. Gerhardt.** 1971. Molecular sieving by the *Bacillus megaterium* cell wall and protoplast. J. Bacteriol. **107:**718–735.
29. **Scherrer, R., L. Louden, and P. Gerhardt.** 1974. Porosity of the yeast cell wall and membrane. J. Bacteriol. **118:**534–540.
30. **Schlosser, D., K. Fahr, W. Karl, and H.-G. Wetzstein.** 2000. Hydroxylated metabolites of 2,4-dichlorophenol imply a Fenton-type reaction in *Gloeophyllum striatum*. Appl. Environ. Microbiol. **66:**2479–2483.
31. **Smith, R. M., A. E. Martell, and R. J. Motekaitis.** 1998. NIST critically selected stability constants of metal complexes database (NIST standard reference database 46). National Institute of Standards and Technology, U.S. Department of Commerce, Gaithersburg, Md.
32. **Srebotnik, E., K. Messner, and R. Foisner.** 1988. Penetrability of white rot-degraded pine wood by the lignin peroxidase of *Phanerochaete chrysosporium*. Appl. Environ. Microbiol. **54:**2608–2614.
33. **Wetzstein, H.-G., N. Schmeer, and W. Karl.** 1997. Degradation of the fluoroquinolone enrofloxacin by the brown rot fungus *Gloeophyllum striatum*: identification of metabolites. Appl. Environ. Microbiol. **63:**4272–4281.
34. **Wetzstein, H.-G., M. Stadler, H.-V. Tichy, A. Dalhoff, and W. Karl.** 1999. Degradation of ciprofloxacin by basidiomycetes and identification of metabolites generated by the brown rot fungus *Gloeophyllum striatum*. Appl. Environ. Microbiol. **65:**1556–1563.
35. **Youngblood, M. P.** 1985. Kinetics of oxidation of triazoliothiohydroquinones by 1,4-benzoquinones: evidence for a hydride-transfer pathway. J. Am. Chem. Soc. **107:**6987–6992.